Electronic Supplementary Material (ESI) for Nanoscale Advances.

Supporting Information

Nucleotide-derived Theranostic Nanodots with Intrinsic Fluorescence and Singlet Oxygen Generation for Bioimaging and Photodynamic Therapy

Xin Ting Zheng, [a] Yee Ching Lai, [b] Yen Nee Tan [a,b,c*]

[a.] *Institute of Materials Research and Engineering (IMRE), Agency for Science, Technology and Research (A*STAR), 2 Fusionopolis Way, Singapore 138634, Singapore*
[b.] *Department of Chemistry, National University of Singapore, 3 Science Drive, Singapore 117543, Singapore*
[c.] *Faculty of Science, Agriculture & Engineering, Newcastle University, Newcastle Upon Tyne NE1 7RU, United Kingdom*
*Corresponding author: [a] tanyn@imre.a-star.edu.sg; [c] yennee.tan@newcastle.ac.uk

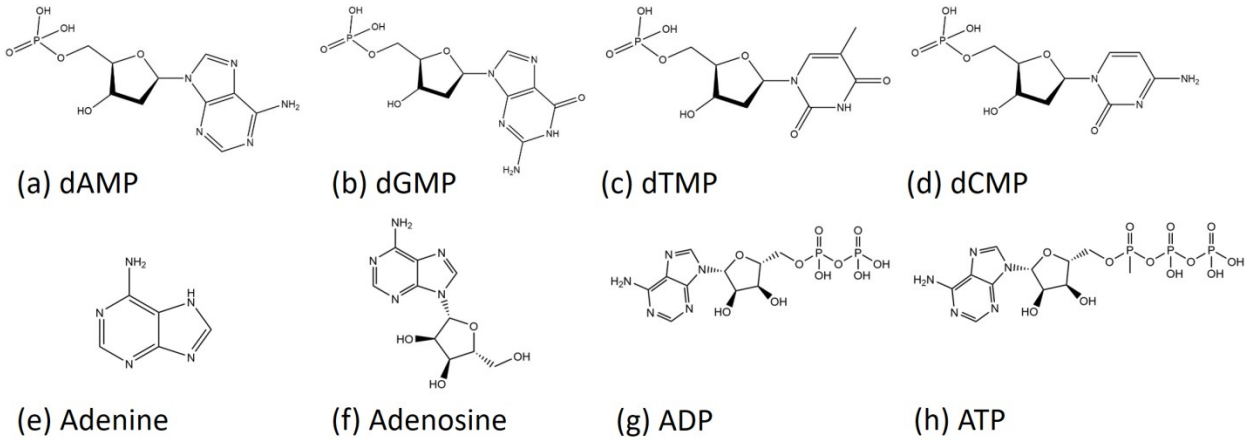

Figure S1. Molecular structure of the four nucleotides and adenine-containing nucleotides precursors (a) dAMP (b) dGMP (c) dCMP (d) dTMP (e) Adenine (f) Adenosine (g) ADP (h) ATP

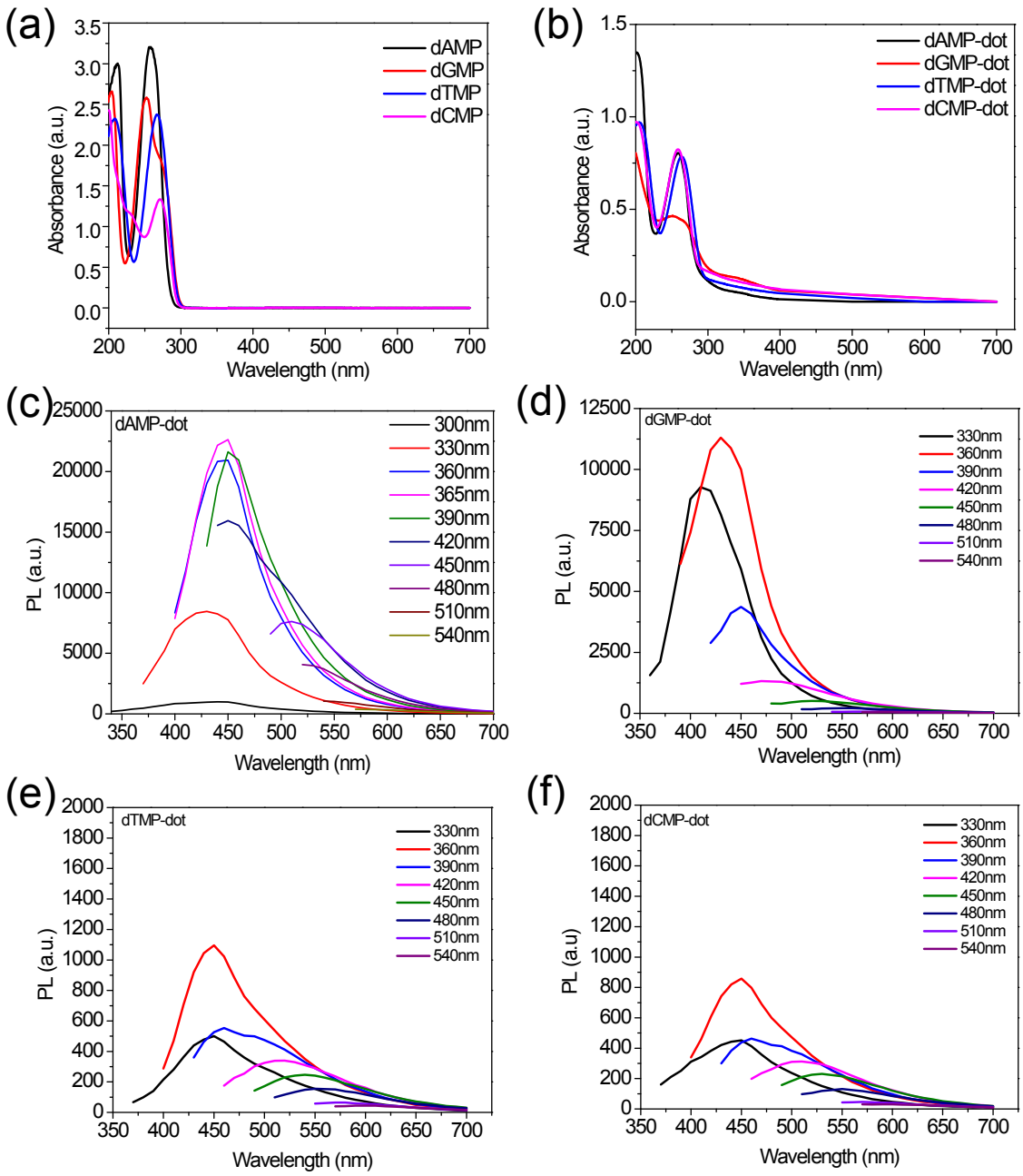

Figure S2. UV-Vis absorption spectra of (a) nucleotides precursors and (b) N-dots; Excitation-dependent photoluminescence spectra of (c) dAMP-dots versus (d) dGMP-dots, (e) dTMP-dots, and (f) dCMP-dots

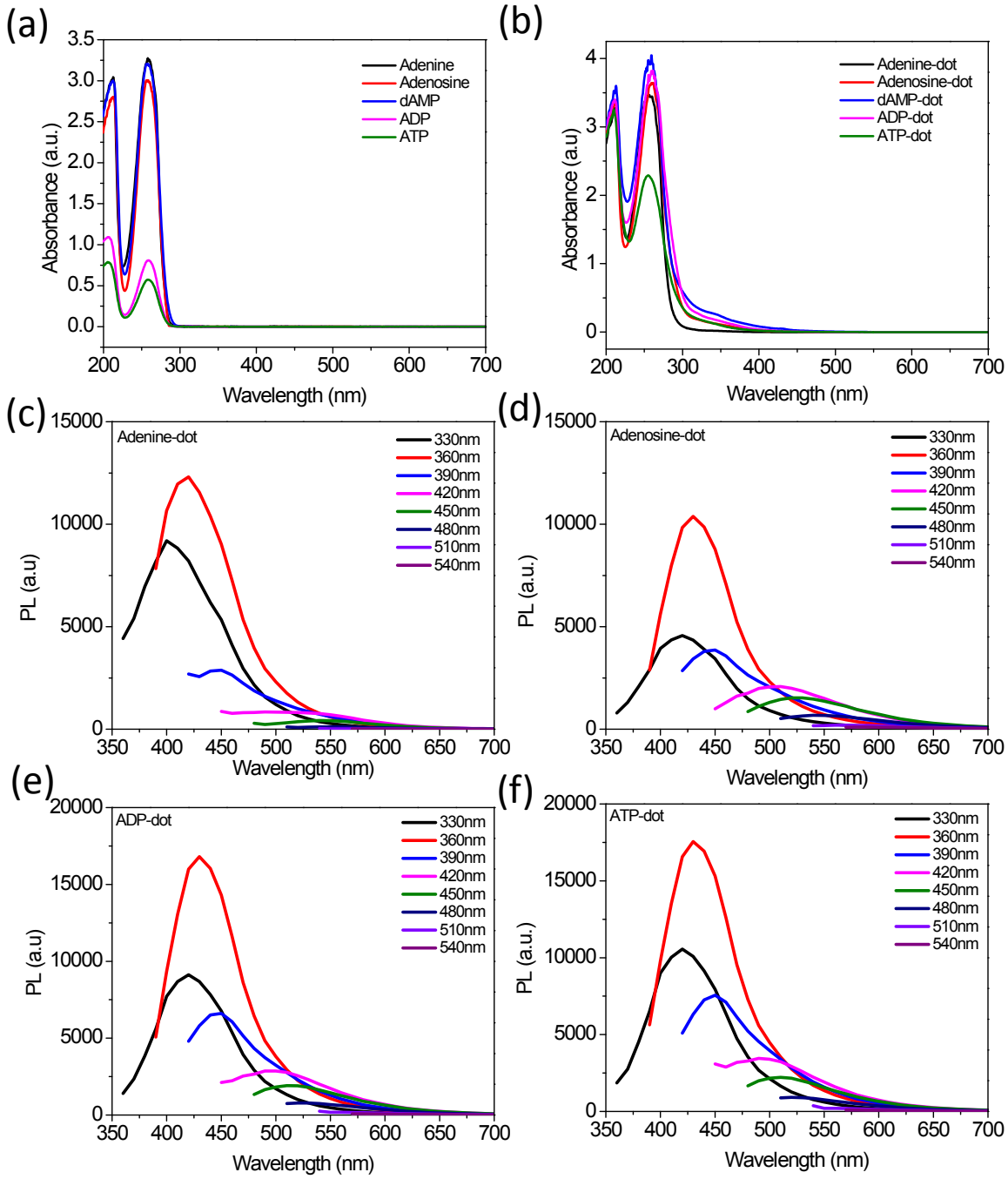

Figure S3. UV-Vis absorption spectra of (a) precursors and (b) A-dots. Excitation dependent photoluminescence Intensity of (c) Adenine, (d) Adenosine, (e) ADP and (f) ATP-dots

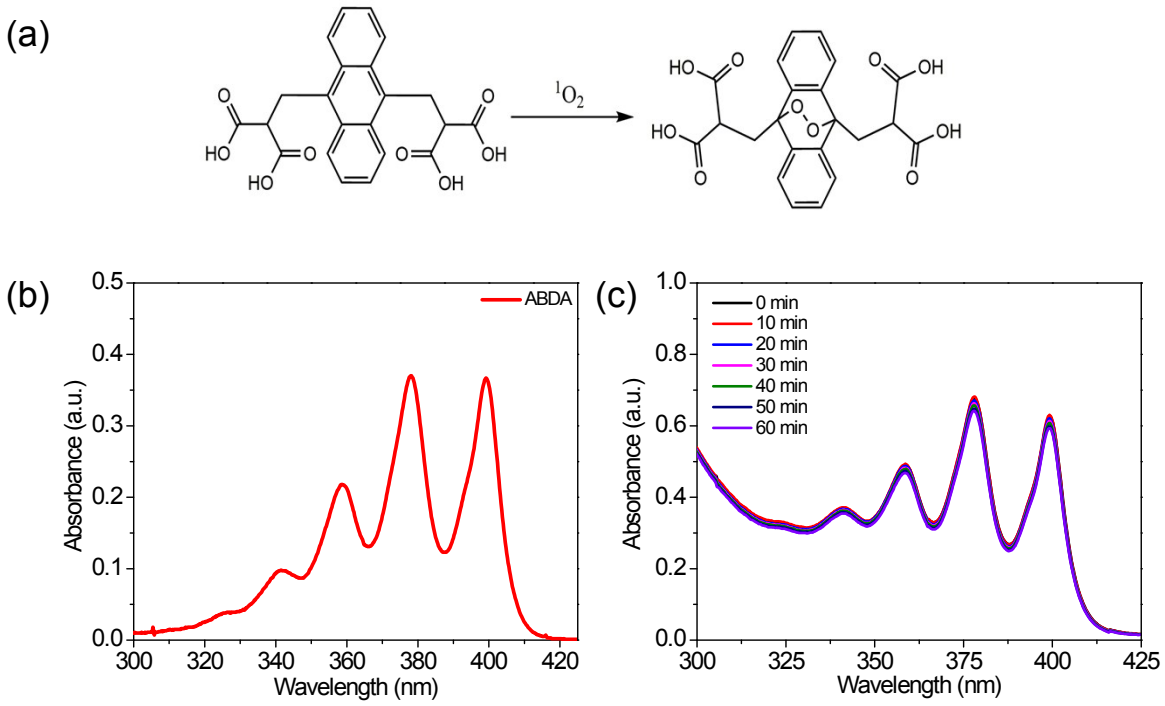

Figure S4. (a) Structure of ABDA and its product after the reaction with singlet oxygen. (b) UV-Vis absorption spectrum of ABDA solution. (c) Time course absorption profile of ABDA showing no generation of singlet oxygen the absence of dAMP-dots

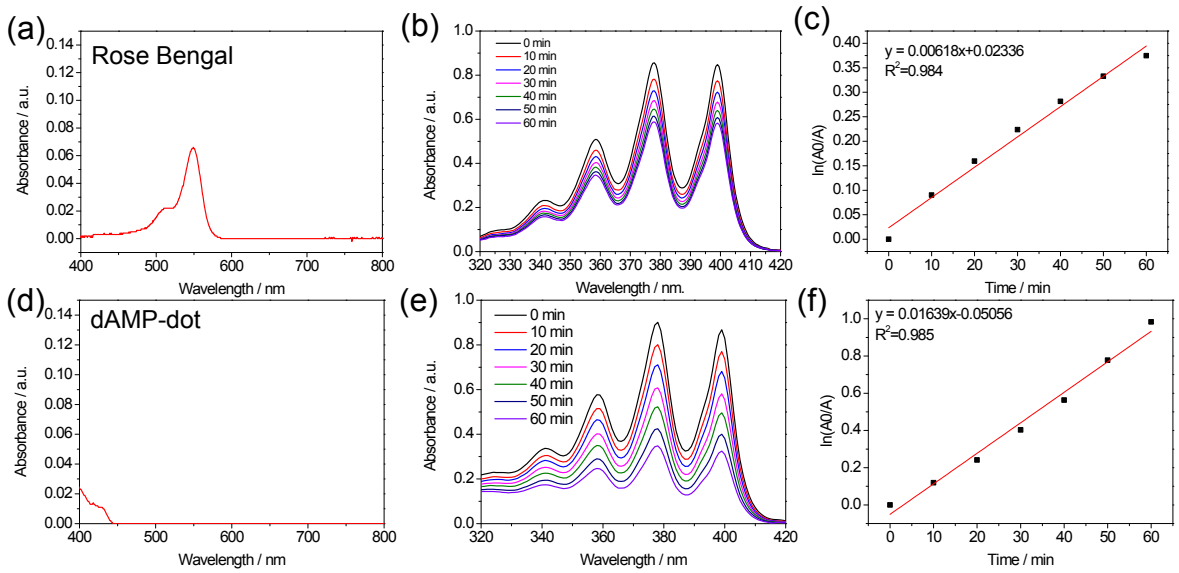

Figure S5. (a) UV-Vis absorption spectrum of Rose Bengal from 400 to 800 nm. (b) Time course absorption spectra of ABDA solution in the presence of Rose Bengal with light. (c) Decomposition rate constant of ABDA in the presence of Rose Bengal with light (d) UV-Vis Absorption spectrum of dAMP-dots from 400 to 800 nm. (e) Time course absorption spectra of ABDA solution in the presence of dAMP-dots with light. (f) Decomposition rate constant of ABDA in the presence of dAMP-dots with light

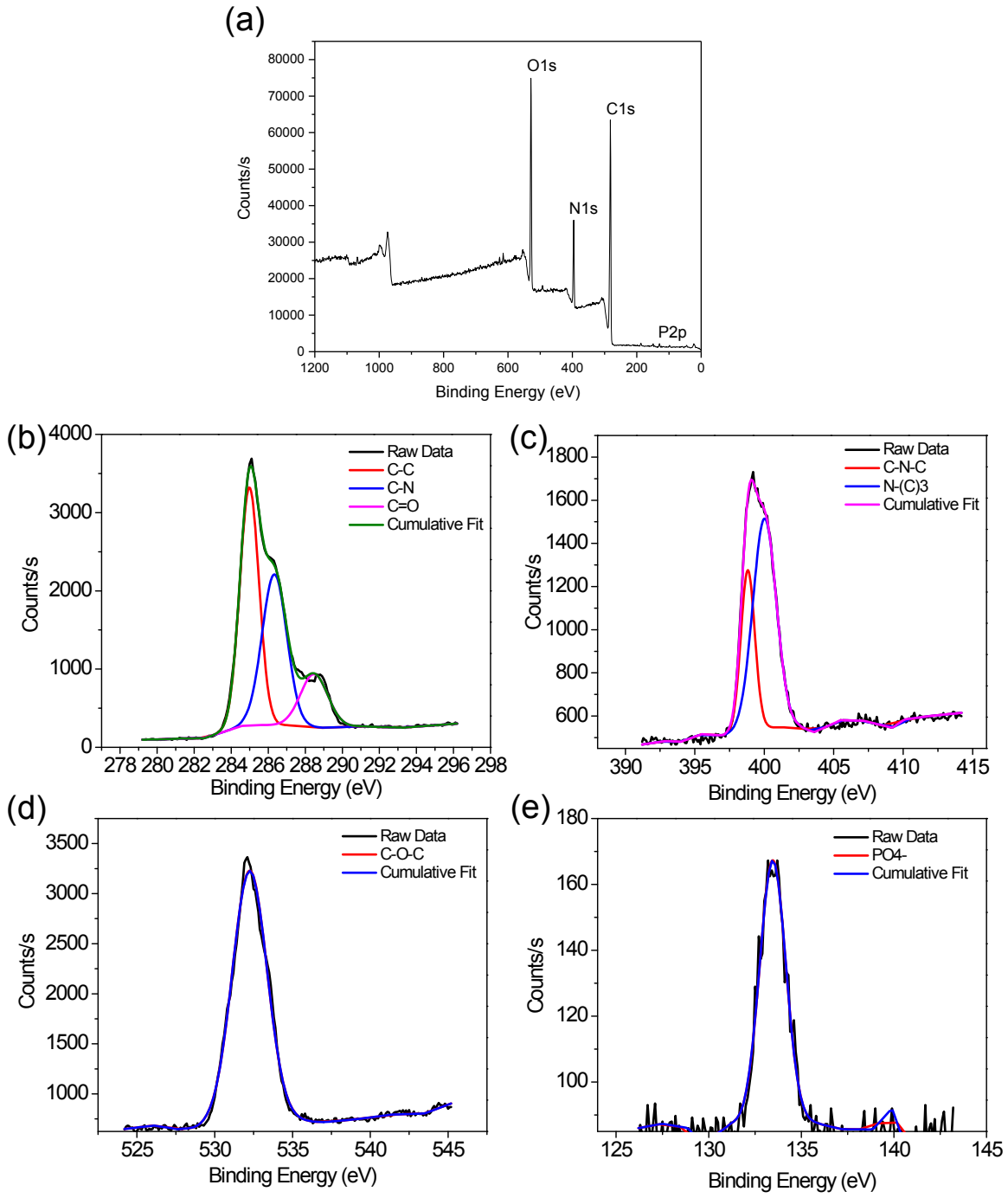

Figure S6. (a) XPS spectrum of dAMP-dots; (b-e) high resolution XPS spectra of (b) C1s,(c) N1s, (d) O1s and (e) P2p

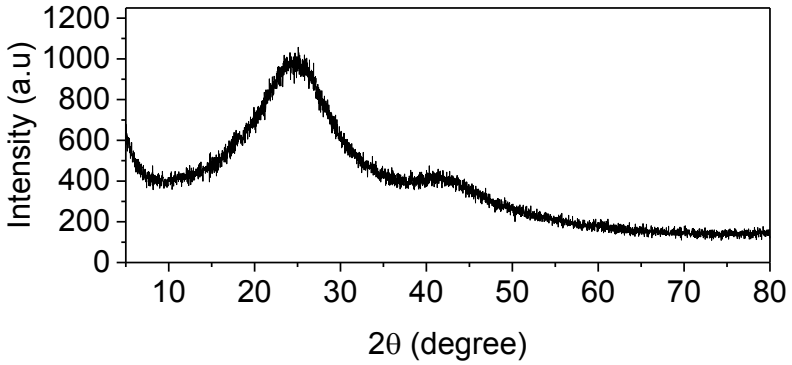

Figure S7. X-ray Diffraction pattern of dAMPdots

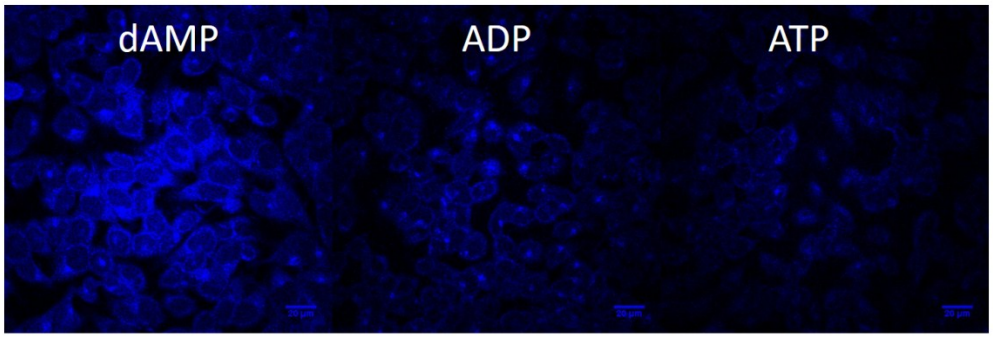

Figure S8. Confocal fluorescence images of dAMP, ADP and ATP-dot treated HeLa cells.

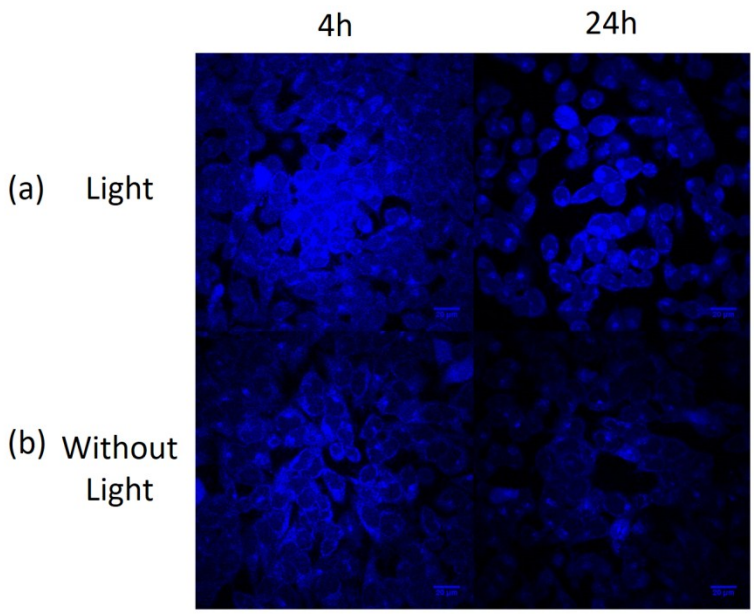

Figure S9. Fluorescence images of Hela cells after 4 h (left column) and 12 h (right column) of incubation in the presence of dAMP-dots (a) with and (b) without light irradiation.

Table S1. Comparison of the intrinsic singlet oxygen generation quantum yield of this work to the reported carbon dot with intrinsic PDT function.

	Carbon source	**Synthesis method**	**Applications**	**Fluorescence quantum yield (%)**	**Singlet oxygen ($^1O_2$) quantum yield**	**Reference**
1	**dAMP**	**Hydrothermal**	**Photodynamic Therapy**	**12.4**	**1.2**	**This work**
2	Graphite rod	Electrochemical etching	Photodynamic Therapy of glioma	Not reported	Not reported	[1]
3	mono-hydroxylphenyl triphenylporphyrin (TPP) and chitosan	Hydrothermal	Photodynamic Therapy of Hepatoma	Not reported	Not reported	[2]
4	Coal	Solvothermal	Nil	47	0.19	[3]
5	Polythiophene benzoic acid (PBA)	Hydrothermal	In vivo Photodynamic and photothermal Therapy	3.5	0.26	[4]
6	3,6-di(2-thienyl)-2,5-dihydropyrrolo(3,4-c)pyrrole-1,4-dione (DPP)	Hydrothermal	Photodynamic Therapy	Not reported	0.276	[5]
7	As-synthesized polythiophene (PT2)	Hydrothermal	In vivo Photodynamic Therapy	Not reported	1.3	[6]

Table S2. Comparison of the fluorescence quantum yield of dAMP dots in this work to the previously reported carbon dots derived from nucleic acid and other precursors

	Carbon source	Synthesis method	Applications	Fluorescence quantum yield (%)	Reference
Dots derived from nucleic acid precursors					
1	**dAMP**	**Hydrothermal**	**Photodynamic Therapy**	**12.4**	**This work**
2	Low molecular weight DNA from salmon	Hydrothermal	Cell imaging	3.65	[7]
3	DNA	Heating	Fe^{3+} sensing	7.5	[8]
4	C_{29}	Hydrothermal	Biothiols and glutathione reductase activity detection	1.1	[9]
Examples of Dots derived from other precursors					
5	D-glucose and L-aspartic acid	Pyrolysis	In vivo fluorescence imaging for noninvasive glioma diagnosis	7.5	[10]
6	Carbon nanopowder	Reflux in nitric acid	Two-photon excited photodynamic therapy	13	[11]
7	α-cyclodextrin	Dehydration using sulphuric acid	Bioimaging and Targeted Photodynamic Therapy	2.1-10.9	[12]
8	Almond husk	High temperature carbonization	Adsorptive removal of pollutant	1.9	[13]
9	Lemon peel	Hydrothermal	Detection of Cr^{6+} in water purification	14	[14]
10	Soot	Hydrothermal	Intracellular trinitrotoluene detection	12.7	[15]
11	Carbon black	Reflux in nitric acid	Bioimaging	4.04	[16]
12	Bithiophene	Ultrasonication	Bioimaging and bacteria killing	10	[17]
13	Amino acids	Hydrothermal	Bioimaging	15-30.44	[18]

References

1. Z. M. Markovic, B. Z. Ristic, K. M. Arsikin, D. G. Klisic, L. M. Harhaji-Trajkovic, B. M. Todorovic-Markovic, D. P. Kepic, T. K. Kravic-Stevovic, S. P. Jovanovic, M. M. Milenkovic, D. D. Milivojevic, V. Z. Bumbasirevic, M. D. Dramicanin and V. S. Trajkovic, *Biomaterials*, 2012, **33**, 7084-7092.
2. Y. Li, X. Zheng, X. Zhang, S. Liu, Q. Pei, M. Zheng and Z. Xie, *Advanced Healthcare Materials*, 2017, **6**, 1600924.
3. M. Li, C. Yu, C. Hu, W. Yang, C. Zhao, S. Wang, M. Zhang, J. Zhao, X. Wang and J. Qiu, *Chemical Engineering Journal*, 2017, **320**, 570-575.
4. J. Ge, Q. Jia, W. Liu, M. Lan, B. Zhou, L. Guo, H. Zhou, H. Zhang, Y. Wang, Y. Gu, X. Meng and P. Wang, *Advanced Healthcare Materials*, 2016, **5**, 665-675.
5. H. He, X. Zheng, S. Liu, M. Zheng, Z. Xie, Y. Wang, M. Yu and X. Shuai, *Nanoscale*, 2018, **10**, 10991-10998.
6. J. Ge, M. Lan, B. Zhou, W. Liu, L. Guo, H. Wang, Q. Jia, G. Niu, X. Huang, H. Zhou, X. Meng, P. Wang, C. S. Lee, W. Zhang and X. Han, *Nat Commun*, 2014, **5**, 4596.
7. C. X. Guo, J. Xie, B. Wang, X. Zheng, H. B. Yang and C. M. Li, *Sci Rep*, 2013, **3**, 2957.
8. G. Cheng, W. Zhang, Y. Zhou, Q. Ge and C. Huang, *Anal. Methods*, 2015, **7**, 6274-6279.
9. Q. H. Li, L. Zhang, J. M. Bai, Z. C. Liu, R. P. Liang and J. D. Qiu, *Biosens Bioelectron*, 2015, **74**, 886-894.
10. M. Zheng, S. Ruan, S. Liu, T. Sun, D. Qu, H. Zhao, Z. Xie, H. Gao, X. Jing and Z. Sun, *ACS Nano*, 2015, **9**, 11455-11461.
11. C. Fowley, N. Nomikou, A. P. McHale, B. McCaughan and J. F. Callan, *Chemical Communications*, 2013, **49**, 8934-8936.
12. Y. Choi, S. Kim, M.-H. Choi, S.-R. Ryoo, J. Park, D.-H. Min and B.-S. Kim, *Advanced Functional Materials*, 2014, **24**, 5781-5789.
13. K. M. Tripathi, A. Tyagi, M. Ashfaq and R. K. Gupta, *RSC Advances*, 2016, **6**, 29545-29553.
14. A. Tyagi, K. M. Tripathi, N. Singh, S. Choudhary and R. K. Gupta, *RSC Advances*, 2016, **6**, 72423-72432.
15. S. Devi, R. K. Gupta, A. K. Paul, V. Kumar, A. Sachdev, P. Gopinath and S. Tyagi, *RSC Advances*, 2018, **8**, 32684-32694.
16. Y. Dong, C. Chen, X. Zheng, L. Gao, Z. Cui, H. Yang, C. Guo, Y. Chi and C. M. Li, *Journal of Materials Chemistry*, 2012, **22**, 8764-8766.
17. K. P. Prasad, A. Than, N. Li, M. Alam Sk, H. Duan, K. Pu, X. Zheng and P. Chen, *Materials Chemistry Frontiers*, 2017, **1**, 152-157.
18. H. V. Xu, X. T. Zheng, Y. Zhao and Y. N. Tan, *ACS Applied Materials & Interfaces*, 2018, **10**, 19881-19888.